Anisotropic Small Angle Light and Neutron Scattering from a Lyotropic Lamellar Phase under Shear

Richard Weigel, Jörg Läuger, Walter Richtering, Peter Lindner

Anisotropic Small Angle Light and Neutron Scattering from a Lyotropic Lamellar Phase under Shear

Richard Weigel ([1]), Jörg Läuger ([1]), Walter Richtering ([1,*])
and Peter Lindner ([2])

([1]) Albert-Ludwigs-Universität Freiburg, Institut für Makromolekulare Chemie und Freiburger Materialforschungszentrum, Stefan-Meier Strasse 31, 79104 Freiburg, Germany
([2]) Institut Max von Laue-Paul Langevin, BP 156, 38042 Grenoble, France

(Received 21 September 1995, received in final form 15 December 1995, accepted 4 January 1996)

PACS.61.30.Eb – Experimental determinations of smectic, nematic, cholesteric, and other structures
PACS.82.70.Dd – Colloids
PACS.83.50.-v – Deformation; material flow

Abstract. — The influence of shear on the lamellar phase of a semi-dilute solution (36% (w/w)) of tetra ethylenglycol dodecylether ($CH_3[CH_2]_{11}[OCH_2CH_2]_4OH$, $C_{12}E_4$) in water was investigated by Small Angle Light Scattering (SALS), Small Angle Neutron Scattering (SANS) and rheology. A plateau modulus was determined by low amplitude oscillatory shear experiments. A strong scattering peak perpendicular to the flow direction and a small peak along the flow direction were observed in rheo-SANS. The rheo-SALS patterns were also anisotropic. At low shear rates, a four lobe pattern was found in depolarized light scattering (H_V) and scattering perpendicular to the flow direction was observed in polarized scattering (H_H). A butterfly pattern was found in light scattering at high shear rates. The butterfly pattern was stable after cessation of shear, but it was changed by slow shear flow. The scattering data can be explained by a shear induced formation of deformed vesicles and the butterfly pattern might be correlated with an assembly of vesicles disordered in the direction of shear.

1. Introduction

Surfactants are known to form lyotropic liquid crystalline phases in concentrated aqueous solution. Different micellar architectures like spheres, rods or disks can exist in isotropic solution and the liquid crystalline phases are characterized by long range orientational order of these micelles. Often hexagonal (H_1) or lamellar (L_α) structures can be observed [1]. Liquid crystalline samples of macroscopic size usually display a polydomain structure which is characterized by a random director orientation. Shear flow is known to have a profound effect on the structure of liquid crystals and the macroscopic alignment of such systems. Rheological properties of lyotropic liquid crystalline materials have been increasingly studied during the last years and always a complex behavior was observed [2–13]. A major problem in rheological studies of anisotropic materials is that the sample structure is often changed during the experiment. In

(*) Author for correspondence (e-mail: rich@ruf.uni-freiburg.de)

other words the linear viscoelastic region can be extremely small and it is difficult to explore whether complex rheological properties are typical of the underlying structure itself or whether they are caused by flow induced structural changes [14, 15]. Information on shear orientation is thus a prerequisite for rheological investigations of lyotropic liquid crystals. Rheo-optical techniques proved to be very helpful in order to study shear alignment and birefringence, small angle light scattering (SALS) and small angle neutron scattering (SANS) have been used e.g. in studies on nematic solutions of stiff macromolecules, elongated micelles or polymeric liquid crystals [16–30]. Often shear thinning was observed which could be correlated e.g. to a tumbling, wagging or flow alignment of the director.

Much less is known about lamellar systems. Roux and coworkers recently studied the effect of shear on a dilute lamellar phase of a multicomponent system and described the results with an orientation diagram [31–33]. At low and high shear rates they observed shear orientation with the layer normal being parallel to the velocity gradient, but formation of multilamellar vesicles was found at intermediate shear rates. Mang *et al.* studied a discotic nematic and lamellar phase of a fluorinated surfactant system and observed an orientation of lamellae with the layer normal being parallel to the neutral (vorticity) axis, i.e. perpendicular to both flow direction and the direction of the velocity gradient [34]. The same kind of shear induced orientation was discussed in a thermotropic smectic phase at high shear rates, but at low shear rates multilamellar cylinders were observed by Panizza *et al.* [35]. Shear alignment of lamellar structures is also known from block copolymer systems. In contrast to lyotropic systems, the lamellae in block copolymer melts are not separated by a solvent and interaction due to entanglements is possible. Again different orientations of lamellae were found in dependence of the conditions of the shear experiment [36, 37].

Obviously, the influence of shear flow on the orientation in lamellar systems can be manifold and investigations of different systems are necessary in order to understand the interaction of mechanical deformation and structural changes.

In this contribution, we present results obtained by means of combined rheo-small angle light scattering (SALS) and rheo-small angle neutron scattering (SANS) experiments from the lamellar phase of aqueous mixtures of the nonionic surfactant $C_{12}E_4$, $CH_3(CH_2)_{11}(OCH_2CH_2)_4OH$. The phase diagram was reported by Mitchell *et al.* and the lamellar phase is stable in a broad concentration and temperature range [38]. Recently, we reported results obtained by rheo-SALS from a concentrated surfactant solution (80% w/w) and shear alignment was observed [39]. Now, we were interested in the behavior of a semi-dilute sample at 36%. At this concentration, the isotropic to lamellar phase transition is observed upon heating. At low temperatures the isotropic phase (L_1) consisting of small micelles and/or vesicles is stable and no long range orientational order is present [38,40]. The L_α phase is reached at room temperature. Thus rheological experiments can be performed in a very convenient temperature range where evaporation of the solvent is not a severe problem. Furthermore, the rheometer can be loaded with the sample being in the isotropic phase and preshearing effects during loading the shear cell can be avoided.

2. Experimental

Synthesis and purification of the surfactant tetraethylenglycol monododecylether (362 g/mol) were performed with standard techniques. Mixtures with H_2O (Millipore Milli-Q plus) were used for the light scattering experiments, but D_2O was used for small angle neutron scattering. The phase transition temperatures decreased by 1-3 K when D_2O was used instead of H_2O. The concentration was 36 and 33.6% (w/w) in normal and heavy water, respectively, which give the same surfactant mol fraction of 0.0272. The ratio of water molecules to ethylene oxide groups was ca. 9.

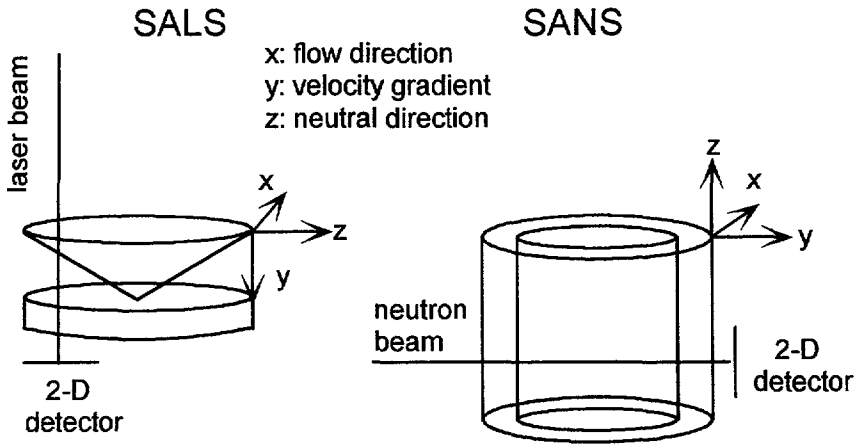

Fig. 1. — Scattering geometries used in SALS and SANS.

A previously described Bohlin stress rheometer with integrated small angle light scattering setup was used for the rheo-optical studies [41]. A HeNe-laser was used as light source and both polarized (H_H) and depolarized (H_V) scattered light were detected with a two-dimensional CCD detector. The largest accessible scattering vector was 4.2 μm^{-1}

The neutron scattering experiments were performed at the instrument D11 of the Institut-Laue-Langevin in Grenoble with a Couette shear cell described previously [42]. The wavelength of the neutrons was 6 Å and the distance between sample and detector was varied between 2.5 and 35.7 m, hence covering a q-range of 0.0015-0.15 $Å^{-1}$

A stress controlled 4 cm/3° cone and plate shear geometry was used in the light scattering experiments and a strain controlled Couette cell with a 1 mm gap was used for neutron scattering. The scattering geometries are shown in Figure 1. The primary beam was in both cases parallel to the direction of the velocity gradient $\nabla \mathbf{V}$ and perpendicular to the flow direction $\mathbf{V}$. The scattering intensity was detected in the plane given by the flow direction and the neutral (vorticity) axis.

3. Results

3.1. Rheological Measurements. — The isotropic phase behaved as a Newtonian liquid and a viscosity of 0.22 Pa s was found at 8 °C. The viscosity in the isotropic phase decreased with temperature and the temperature dependency was of Arrhenius type, but the viscosity increased when the lamellar phase was approached at 17 °C. The lamellar phase showed elastic properties. A plateau modulus of 100 Pa was determined in low amplitude oscillatory shear experiments. Elastic properties were also found in creep curves, but shear thickening at short and shear thinning at long creep times were observed. The viscosity determined after long shear times first decreased with shear stress, then a plateau was observed at intermediate shear stresses (1-10 Pa) which was followed by shear thinning again at stresses above 10 Pa.

3.2. Small Angle Neutron Scattering (SANS). — A radially isotropic small angle neutron scattering intensity was observed with the isotropic and lamellar phases in the quiescent state. Figure 2 displays the angular dependence of the radially averaged intensity, the scattering vector q is given as $q = (4\pi/\lambda)\sin(\theta/2)$ with λ the neutron wavelength and θ the scattering angle. A peak was observed in both phases, but the position of the maximum was different:

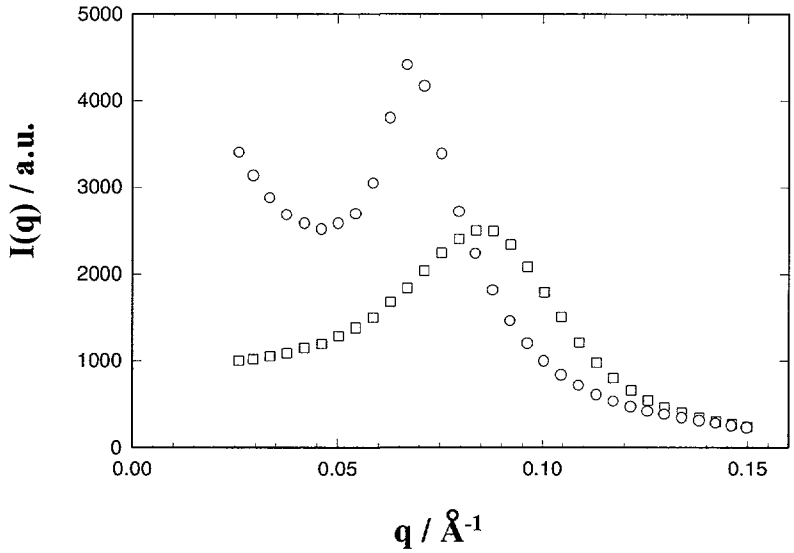

Fig. 2. — Angular dependence of SANS intensity: (□) isotropic phase (8 °C) at rest and (○) lamellar phase (25 °C) at rest, prior to shearing.

$q_{max} = 8.4\times10^{-2}$ Å^{-1} in the L_1 phase and $q_{max} = 6.9\times10^{-2}$ Å^{-1} in the L_α phase. Additionally, small angle scattering was detected in the lamellar phase but not in the isotropic L_1 phase.

Shear flow had no influence on the SANS pattern in the isotropic phase. However, the intensity distribution on the two-dimensional detector became anisotropic in the lamellar phase under shear. Figure 3 shows contour plots at different shear rates and the angular dependence of the intensity radially averaged in a sector along and perpendicular to the flow direction is shown in Figure 4 for some shear rates. The scattering intensity in the direction perpendicular to the flow direction was higher compared to the scattering intensity along the flow direction. The position of the maximum was the same in both directions and shifted to slightly larger q-values at high shear rates with $q_{max} = 7.7\times10^{-2}$ Å^{-1} at $\dot{\gamma} = 840$ s^{-1}. The intensity maximum along the flow direction, however, was rather weak at high shear rates. The q-dependence of the intensity 15 min after cessation of shear is also displayed in Figure 4. The total scattering intensity increased after cessation of shear and the intensity maximum along the flow direction recovered.

A second series of measurements was performed at a longer sample-to-detector distance in order to study the effect of shear in the low q-range. Again the intensity distribution became anisotropic under shear and the scattering intensity perpendicular to flow direction was higher as compared to the parallel direction, see Figure 5. A small peak perpendicular to the flow direction was observed after cessation of flow at 840 s^{-1}

3.3. Rheo-Small Angle Light Scattering (SALS) . — Rheological measurements revealed shear thinning at low shear stresses. A viscosity plateau was found at intermediate stresses and shear thinning was observed again at stresses larger than 10 Pa. Simultaneously, small angle light scattering was detected and both polarized (H_H) and depolarized (H_V) scattered intensity are shown in Figure 6. The H_V intensity was much weaker than the H_H intensity. Typically, the exposure time of the CCD camera was four times longer in H_V as compared to H_H scattering. A four lobe pattern was observed in depolarized scattered light at low shear

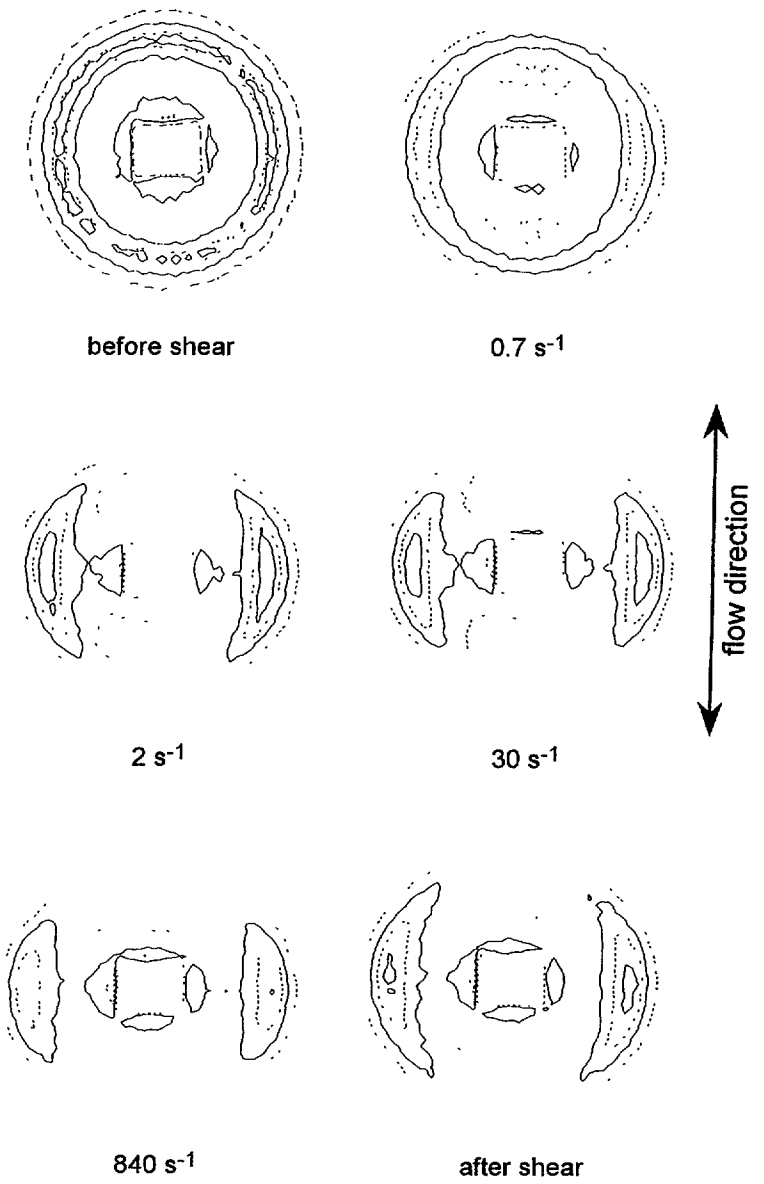

Fig. 3. — Contour plots of the SANS intensity from the lamellar phase at different shear rates.

stresses, which correspond to the viscosity plateau, but an enhanced scattering intensity in the direction of flow was observed at higher stresses i.e. in the shear thinning region. The polarized scattered light showed a different behavior at low shear stress. An anisotropic pattern was found, where scattered light was detected mainly in the direction perpendicular to the flow direction. At high shear stress, enhanced scattering intensity in the flow direction was observed like in depolarized scattering. The same scattering pictures were obtained when shear stress was decreased, i.e. a four lobe pattern in H_V and scattering perpendicular to the flow direction in H_H scattering were observed again at low stresses.

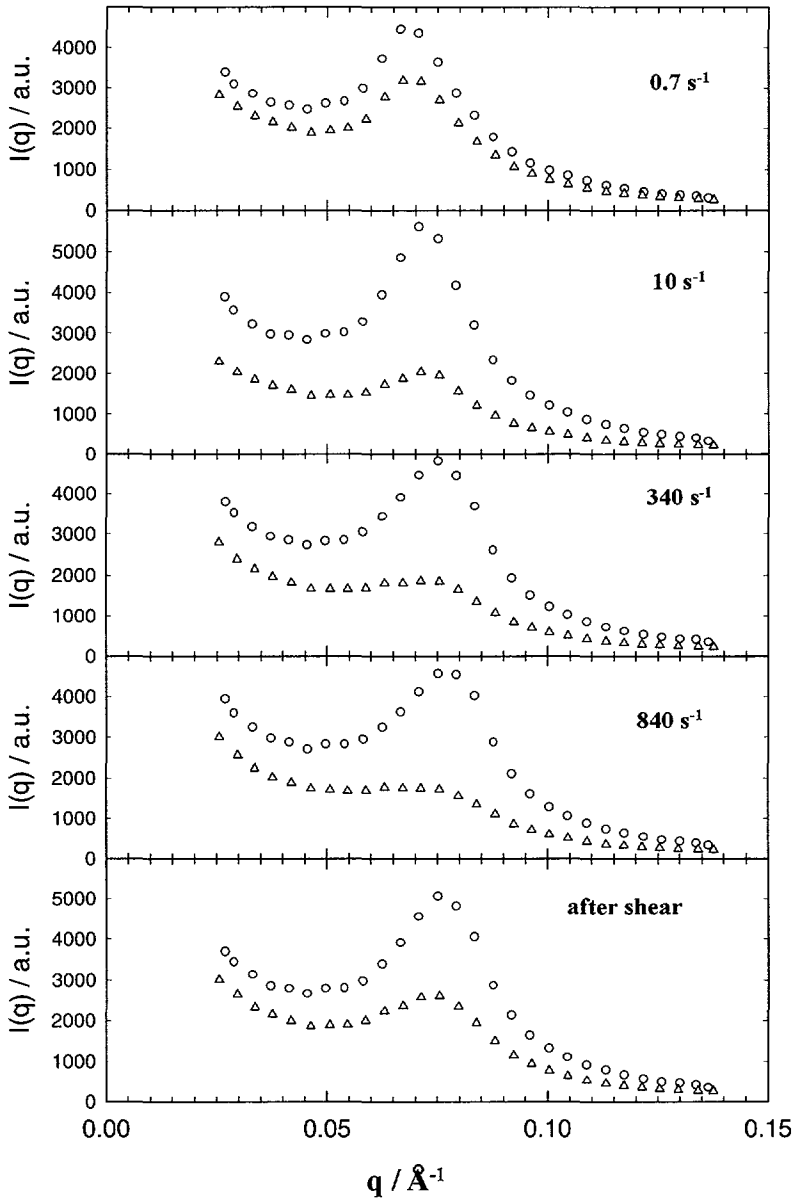

Fig. 4. — Angular dependence of SANS intensity from the lamellar phase at different shear rates, perpendicular (○) and parallel (△) to the flow direction.

4. Discussion

SANS at large scattering vectors probes dimensions on the micellar length scale (typically 2-20 nm) and the thickness of the double layer can be obtained from the position of the intensity maximum in the isotropic L_1 phase. The q_{max}-value corresponds to 7.5 nm. This value was not affected by shear flow.

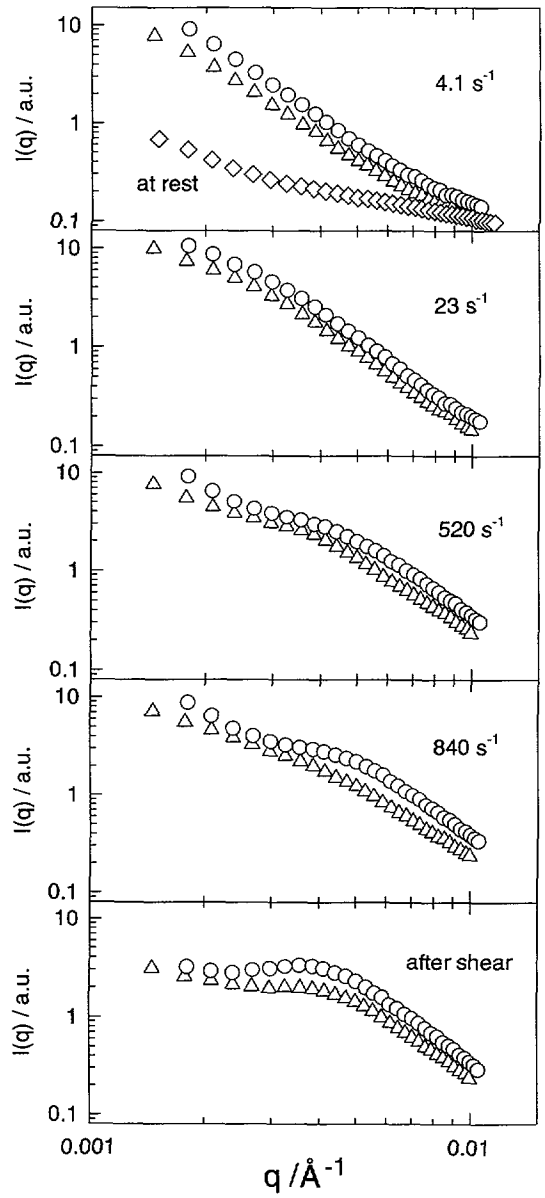

Fig. 5. — Angular dependence of SANS intensity in the small-q-region from the lamellar phase at different shear rates, perpendicular (○) and parallel (△) to the flow direction. The first plot also shows the intensity from the sample before shear (◊).

The lamellar spacing obtained from q_{max} in the L_α phase was 9.1 nm. The isotropic intensity distribution on the two-dimensional multidetector is characteristic for a powder spectrum which is typical of a sample with a polydomain structure. In other words there was no homogeneous orientation of the surfactant double layers. In lamellar systems often a preferred orientation of lamellae parallel to the walls is observed in thin specimen. However, the gap size in the

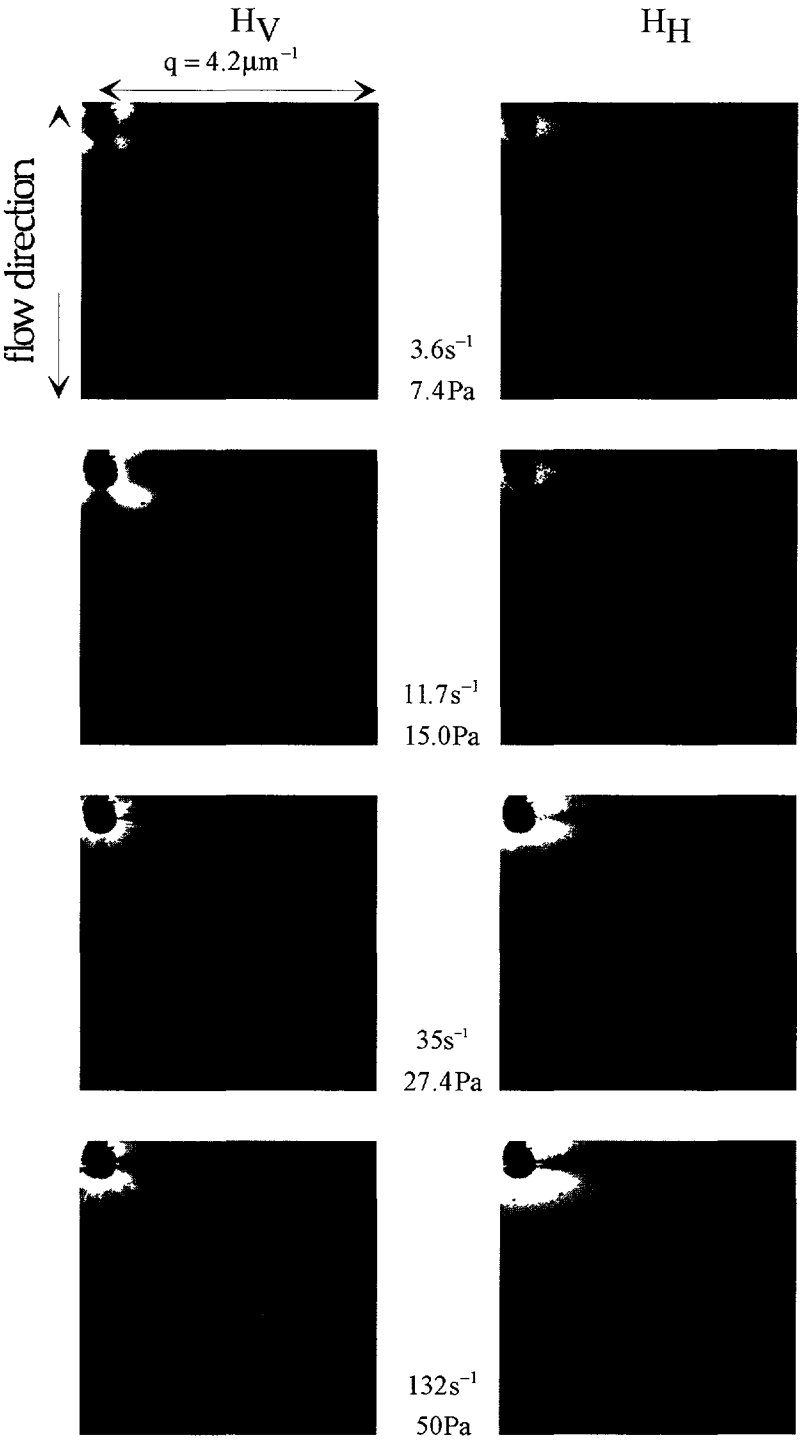

Fig. 6. — Depolarized (left) and polarized (right) SALS patterns from the lamellar phase under shear at increasing shear stresses. The primary beam, hidden by a beam stop, is in the upper left corner.

couette cell was 1 mm, which is sufficiently large in order to avoid wall effects. The small angle scattering is caused by concentration and layer displacement fluctuations that are typical of samples with polydomain structure [43].

The orientation distribution of lamellae changed when a shear deformation was applied. A strong peak was observed perpendicular to the flow direction i.e. along the neutral direction, indicating a preferred stacking of lamellae in the neutral direction. However, a weaker scattering peak was also observed along the flow direction and thus the orientation of surfactant double layers was preferentially perpendicular to the flow direction, but not exclusively.

Diat *et al.* recently studied the effect of shear on a dilute lamellar phase with a larger layer spacing [31–33]. They observed three different regimes: at low and high shear rates the lamellae were aligned parallel to the walls, in other words the layer normal was parallel to the velocity gradient. At intermediate shear rates, formation of multilamellar vesicles was observed. The low shear rate orientation was not found in this study, which indicates that the lowest shear rate applied here was already too high. Rheo-NMR studies by Lukaschek *et al.* showed that an orientation of lamellae parallel to the walls can be observed in this system only at shear rates much smaller than 1 s^{-1} [44].

Vesicular structures (i.e. corresponding to state II in the orientation diagram presented by Diat *et al.* [33]) could explain our neutron scattering data. Vesicles consist of closed bilayers and usually they are of spherical shape. Shear deformation, however, can deform the vesicles. Such anisotropic particles will align with their long axis in flow direction and therefore a higher fraction of bilayers is oriented with the layer normal perpendicular than parallel to the flow direction. The vesicles observed by Roux and coworkers had diameters of several micrometers and they were only slightly deformed. Our neutron scattering data, however, indicate a strong deformation, which is probably due to a different effective volume fraction of the vesicles and a different elastic constant of the bilayer. The surfactant concentration in our system was much higher as compared to the system studied by Diat *et al.* The different water content also results in a shorter distance between double layers.

The different shape is also reflected in the light scattering patterns. Roux *et al.* observed a ring in their SALS experiments which is typical of large spheres [33]. Different behavior was found in our case as can be seen in Figure 6. At low shear rates, enhanced scattering perpendicular to the flow direction was observed in polarized scattering, whereas a four lobe pattern (like a four-leaf clover) was found in depolarized scattering. Scattering probes dimensions in reciprocal space and scattering of the longer axis of an elongated particle is detected at small scattering angles, whereas the shorter axis gives rise to scattering at higher angles. Elongated objects are usually aligned with their long axis along the flow direction and therefore scattering mainly perpendicular to the direction of flow is observed, if the accessible q-vectors are too large in order to detect scattering from the longer axis. Thus deformed vesicles can explain the H_H scattering patterns displayed in Figure 6.

A four lobe scattering pattern as found in depolarized light scattering at low shear rates is observed with optically anisotropic particles [45, 46]. Optically anisotropic particles are e.g spherulites, but deformed vesicles could also give rise to a four lobe depolarized scattering pattern. Light scattering is caused by fluctuations in polarizability. The polarizability of the surfactant molecule in the double layer is different in the directions parallel and perpendicular to the molecular axis. The orientation of surfactant molecules in a vesicle, however, is inhomogeneous, see Figure 7. In that part of the vesicle's double layer, that corresponds to the short axis, the surfactant molecules are aligned with their molecular axis along the flow direction and therefore this part of the double layer has a different polarizability in the polarization plane of the primary laser beam as compared to the bilayer in the longer axis of the vesicle. This internal structure could explain the observed four lobe pattern. The four lobe pattern extends

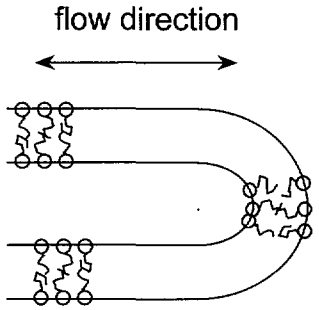

Fig. 7. — Schematic diagram of a surfactant double layer in vesicles.

to higher scattering angles at 15 Pa as compared to scattering at 7.4 Pa, indicating that the vesicles were smaller at the higher shear stress. This proposed structure is supported by the SANS data. SANS revealed a preferred stacking of lamellae in the neutral direction and the surfactant molecules are aligned along the neutral axis. However, neutron scattering due to the double layer was also observed along the flow direction indicating that vesicles with closed bilayers were present.

The depolarized scattering intensity of anisotropic spherical objects can be calculated as [46]:

$$I_{\mathrm{Hv}} = A\rho^2 V_0^2 (3/U^3)^2 \left\{(\alpha_{\mathrm{t}} - \alpha_{\mathrm{r}}) \left[\cos^2(\theta/2)/\cos\theta\right] \sin\mu\cos\mu(4\sin U - U\cos U - 3\mathrm{Si}\ U)\right\}^2 \quad (1)$$

with V_0 volume of the anisotropic sphere; α_{t} and α_{r} are the tangential and radial polarizabilities of the sphere; θ and μ are the radial and azimuthal scattering angles; A is a proportionality constant; Si U is the sine integral; ρ a geometric polarization correction term and U is the sphere shape factor $U = q \cdot R$ with sphere radius R. A four lobe pattern is observed with an intensity maximum at [47,48]:

$$U_{\max} = Rq_{\max} = 4.1 \quad (2)$$

The $\mathrm{H_V}$ pattern at a low shear rate of 3.6 $\mathrm{s^{-1}}$ can be approximately described as symmetrical and a vesicle radius of ca. 10 μm can be estimated from the scattering intensity. At higher shear rates the four lobe pattern was clearly anisotropic indicating the deformation of the vesicles. Additionally, scattering intensity was detected at larger q-vectors, thus the vesicle size decreased. In the case of oriented monodisperse ellipsoides, the shape factor U was given by Stein and Wilkes as [48]:

$$U_{\mathrm{ellipsoid}} = q\left[1 + (\nu^2 - 1)\cos^2(\theta/2)\cos^2\mu\right] \quad (3)$$

with axis ratio ν. The depolarized scattering intensity can be calculated if one assumes equation (1) to be also valid for ellipsoides. Anisotropic four lobe patterns with a similar shape as observed experimentally at a shear rate of 11.7 $\mathrm{s^{-1}}$ were calculated with a longer half axis of 7 μm and an aspect ratio of two. Four lobe patterns for anisotropic rods were obtained by Moritani *et al.* [49]. A quantitative comparison between simulated and experimental SALS patterns, however, is rather difficult, because effects of polydispersity both in size and shape of the deformed vesicles can influence the intensity distribution. Since the vesicles are formed from sheared lamellae in concentrated solution, the size and the number of bilayers can be expected to be polydisperse. Furthermore, the effect of shear forces on the elongation of the vesicles can also depend on the vesicle size. Nevertheless, the observation of an anisotropic

four lobe pattern at larger scattering vectors indicates that an increase of shear rate lead to a stronger average deformation of the vesicles and the mean size decreased.

At higher shear rates, enhanced scattering in flow direction was found in polarized and depolarized light scattering. Here no scattering intensity was detected in the direction perpendicular to the flow. This characteristic scattering pattern has been observed before and was termed "butterfly" pattern. Butterfly scattering patterns have been observed in many different systems including semi-dilute polymer solutions, polymer networks, mixtures of molten polymers, liquid crystals and polymer liquids filled with silica spheres [50–57]. The butterfly pattern is believed to arise from shear induced concentration and orientation fluctuations and might be a universal feature of soft two-component solids [58, 59]. The butterfly pattern observed in this study was rather stable, and it was observed for a long time after cessation of flow at high shear rates (the observation was stopped after 90 minutes). Usually butterfly patterns relax within a few seconds. The stability of the butterfly pattern after cessation of flow might indicate that a different structure was induced by shear which was also stable without shear flow. On the other hand, the scattering pattern changed when the sample was sheared at low shear rates. In other words, the shear induced structure was destroyed by slow shear flow.

The structure that is responsible for the butterfly pattern is difficult to determine. The neutron scattering experiments covered the range of shear rates where the light scattering pattern changed. Neutron scattering, however, revealed enhanced scattering perpendicular to the flow direction in the entire investigated q-range at all shear rates. Obviously, the structure responsible for the butterfly pattern observed in light scattering was not detected by neutron scattering. DeGroot *et al.* recently observed a butterfly pattern in SALS from polymer melts filled with silica particles [55]. The size of the particles was much smaller than the typical length scale that is observed with light scattering and the butterfly pattern was explained with clusters built of flocculated silica particles. In shear flow, these clusters were compressed in the flow direction, which could cause different refractive indices along and perpendicular to the flow direction, respectively. A shear induced concentration fluctuation in a concentrated solution of vesicles is also conceivable in our case, but it would not explain why the butterfly pattern remained stable after cessation of flow. Usually butterfly patterns were observed from samples without long range order such as polymer solutions or the above mentioned filled polymer melt. The surfactant solution studied here, however, revealed an internal structure as can be seen from the SALS and SANS data. The butterfly in this case therefore does not characterize a transition from a homogeneous sample to a sample with shear induced concentration fluctuations. Instead an already shear aligned structure was altered and apparently the degree of order was decreased. A lower degree of order could also explain that the SANS peak along the flow direction became weaker at high shear rates.

The new structure still had elastic properties and low amplitude oscillatory shear experiments revealed a frequency independent storage modulus of 150 Pa that was much higher than the loss modulus (10 Pa). This high (shear induced) elasticity could be a reason why the butterfly pattern was stable after cessation of flow. The underlying structure could still consist of vesicles. Hoffmann *et al.* recently showed that concentrated solutions of vesicles have a high plateau modulus [60,61]. This comparison might indicate, that the butterfly pattern was caused by a disordered assembly of elongated vesicles. Such a change in the arrangement would not influence the neutron scattering data at high scattering vector. The SANS data at low q-vector changed somewhat at high shear rates and after cessation of flow a small peak was detected in the neutral direction. This peak could indicate the formation of a regular structure in the neutral direction, Figure 5. A homogenous structure perpendicular to the flow direction would explain the absence of scattered light in the neutral direction and would lead to the butterfly

pattern. However, SANS measurements in a broader q-range are necessary in order to check this assumption.

A comparison of our results with the data of Diat *et al.* [31–33] indicates that the measurements presented here correspond to the vesicular structure of region II. Rheo-NMR experiments by Lukaschek *et al.* showed that, at a concentration of 35% (w/w) $C_{12}E_4$ in D_2O, region I (lamellae oriented parallel to the walls) can only be obtained at shear rates much lower than 1 s^{-1} [44]. Such low shear rates were not used in this study.

However, there are some differences in the behavior of the concentrated surfactant solutions investigated here if compared to region II of the dilute lamellar phase studied by Roux *et al.* [31–33]. i) A viscosity plateau was observed before the onset of shear thinning, ii) SANS gave indications for the presence of strongly elongated vesicles. iii) Most strikingly, however, is the difference in the SALS patterns. Roux *et al.* observed a scattering ring independent of shear rate which is typical of spherical vesicles. In our case the SALS pattern changed with shear rate. At low shear rates, the scattering pictures can be explained by oriented elongated vesicles. At high shear rates, the existence of enhanced concentration fluctuations along the flow direction was indicated by a butterfly pattern.

Previously reported rheo-SALS experiments with a surfactant concentration of 80% revealed different behavior as compared to Figure 6 [39]. The different scattering pictures demonstrate that the surfactant concentration, or in other words the bilayer distance, has a profound influence of shear induced structures. Obviously, there is not sufficient water available for the formation of vesicles at a surfactant concentration of 80%. Vesicles can be formed at 36% with an average size of a few μm. They become smaller with increasing shear rate and eventually the scattering is dominated by a butterfly pattern indicating the formation of a suprastructure consisting of vesicles. This influence of surfactant concentration was also found by Lukaschek *et al.* [44] and a presence of stable vesicles in dilute aqueous solutions of $C_{12}E_4$ was observed by Olsson *et al.* [40]. Finally, we wish to note that SALS patterns similar to those described here were also found in a lamellar three component system at a similar water content [62]. More experiments are necessary to obtain a complete understanding of the influence of shear on lyotropic lamellar systems. Especially scattering experiments covering a broad q-range seem to be interesting in order to characterize the structure responsible for the butterfly pattern.

5. Summary and Conclusion

The influence of shear on the lamellar phase at a concentration of 36% (w/w) $C_{12}E_4$ in water was investigated by SALS and SANS. The employed shear rates correspond to the region where shear induced vesicles exist (region II in the notation of Roux *et al.*) [33]. The higher surfactant concentration as compared to the study by Roux *et al.* influenced the solution structure. The particles were deformed and aligned in the shear flow. At high shear rates the viscosity decreased and a butterfly pattern was observed in light scattering indicating a vesicular structure that was disordered in the flow direction, but homogeneous in the neutral (vorticity) direction. The butterfly pattern was stable after cessation of flow, but disappeared in slow shear flow.

Acknowledgments

Support by the Deutsche Forschungsgemeinschaft is gratefully acknowledged. We thank Jörg Berghausen for assistance with rheological measurements.

References

[1] Tiddy G.J.T., *Phys. Rep.* **57** (1980) 1.
[2] Solyom P. and Ekwall P., *Rheol. Acta* **8** (1969) 316.
[3] Oswald P. and Allain M., *J. Phys. France* **46** (1985) 831.
[4] Matsumoto T., Heiuchi T. and Horie K., *Colloid Polym. Sci.* **267** (1989) 71.
[5] Paasch S., Schambil F. and Schwuger M.J., *Langmuir* **5** (1989) 1344.
[6] Cates M.E. and Milner S.T., *Phys. Rev. Lett.* **62** (1989) 1856.
[7] Valdés M., Manero O., Soltero J.F.A. and Puig J.E., *J. Colloid Interface Sci.* **160** (1993) 59.
[8] Robles-Vásquez O., Corona-Galván S., Soltero J.F.A., Puig J.E., Tripodi S.B., Vallés E. and Manero O., *J. Colloid Interface Sci.* **160** (1993) 65.
[9] Lu C.-Y.D. and Cates M.E., *J. Chem. Phys.* **101** (1994) 5219.
[10] Alcantara M.R. and Vanin J.A., *Colloids Surf.A* **97** (1995) 151.
[11] Soltero J.F.., Rables-Vásquez O., Puig J.E. and Manero O., *J. Rheol.* **39** (1995) 235.
[12] Franco J.M., Munoz J.M. and Gallegos C., *Langmuir* **11** (1995) 669.
[13] Richtering W., Läuger J. and Linemann R., *Langmuir* **10** (1994) 4374.
[14] Hoffmann H., Hofmann S., Rauscher A. and Kalus J., *Progr. Colloid Polym. Sci.* **84** (1991) 24.
[15] Linemann R., Läuger J., Schmidt G., Kratzat K. and Richtering W., *Rheol. Acta* **34** (1995) 440.
[16] Cummins P.C., Staples E., Hayter J.B. and Penfold J., *J. Chem. Soc. Farady Trans. I* **83** (1987) 2773.
[17] Moldenaers P., Fuller G.G. and Mewis J., *Macromolecules* **22** (1989) 960.
[18] Takebe T., Hashimoto T., Ernst B., Navard P. and Stein R.S., *J. Chem. Phys.* **92** (1990) 1386.
[19] Larson R.G. and Doi M., *J. Rheol.* **35** (1991) 539.
[20] Safinya C.R., Sirota E.B. and Plano R.J., *Phys. Rev. Lett.* **66** (1991) 1986.
[21] Kalus J. and Schmelzer U., *Trends Phys. Chem.* **3** (1992) 299.
[22] Münch C., Hoffmann H., Kalus K.I.J., Neubauer G., Schmelzer U. and Selbach J., *J. Phys. Chem.* **97** (1993) 4514.
[23] Berret J.F., Roux D.C., Porte G. and Lindner P., *Europhys. Lett.* **25** (1994) 521.
[24] Dadmun M.D. and Han C.C., *Macromolecules* **27** (1994) 7522.
[25] Hamilton W.A., Butler P.D., Baker S.M., Smith G.S., Hayter J.B., Magid L.J. and Pynn R., *Phys. Rev. Lett.* **72** (1994) 2219.
[26] Kannan R.M. and Kornfield J.A., *J. Rheol.* **38** (1994) 1127.
[27] Bedford B.D. and Burghardt W.R., *J. Rheol.* **38** (1994) 1656.
[28] Berret J.-F. and Roux D.C., *J. Rheol.* **39** (1995) 725.
[29] Schmitt V., Schosseler F. and Lequeux F., *Europhys. Lett.* **30** (1995) 31.
[30] Richtering W., Schmidt G. and Lindner P., *Colloid Polym. Sci.* **274** (1996) 85.
[31] Diat O. and Roux D., *J. Phys. II France* **3** (1993) 9.
[32] Roux D., Nallet F. and Diat O., *Europhys. Lett.* **24** (1993) 51.
[33] Diat O., Roux D. and Nallet F., *J. Phys. II France* **3** (1993) 1427.
[34] Mang J.T., Kumar S. and Hammouda B., *Europhys. Lett.* **28** (1994) 489.
[35] Panizza P., Archambault P. and Roux D., *J. Phys. II France* **5** (1995) 303.
[36] Koppi K.A., Tirrell M., Bates F.S., Almdal K. and Colby R.H., *J. Phys. II France* **2** (1992) 1941.
[37] Patel S.S., Larson R.G., Winey K.I. and Watanabe H., *Macromolecules* **28** (1995) 4313.
[38] Mitchell D.J., Tiddy G.J.T., Waring L., Bostock T. and McDonald M.P., *J. Chem. Soc*

Faraday Trans. I **79** (1983) 975.
[39] Läuger J., Linemann R. and Richtering W., *Rheol. Acta* **34** (1995) 132.
[40] Sarrazin-Cartalas A., Iliopoulos I., Audebert R. and Olsson U., *Langmuir* **10** (1994) 1421.
[41] Läuger J. and Gronski W., *Rheol. Acta* **34** (1995) 70.
[42] Lindner P. and Oberthür R.C., *Rev. Phys. Appl.* **19** (1984) 759.
[43] Marignan J., Appell J., Basserau P., Porte G. and May R., *J. Phys. France* **50** (1989) 3553.
[44] Lukaschek M., Müller S., Hasenhindl A., Grabowski D. A. and Schmidt C., *Colloid Polym. Sci.* **274** (1996) 1.
[45] Clough S., van Aartsen J.J. and Stein R.S., *J. Appl. Phys.* **36** (1965) 3072.
[46] Samuels R.J., *J. Polym. Sci. Part A-2* **9** (1971) 2165.
[47] Stein R.S. and Rhodes M.B., *J. Appl. Phys.* **31** (1960) 1873.
[48] Stein R.S. and Wilkes G.L., in "Structure and Properties of Oriented Polymers", I. M. Ward Ed. (Appl. Sci. Publ., London, 1975).
[49] Moritani M., Hayashi N., Utsuo A. and Kawai H., *Polym. J.* **2** (1971) 74.
[50] Oeser R., Picot C. and Herz J., Polymer motion in dense systems, Springer Proceedings in Physics **29** (1988).
[51] Bastide J., Leibler L. and Prost J., *Macromolecules* **23** (1990) 1821.
[52] Inoue T., Moritani M., Hashimoto T. and Kawai H., *Macromolecules* **4** (1971) 500.
[53] van Egmond J.W. and Fuller G.G., *Macromolecules* **26** (1993) 7182.
[54] Moses E., Kume T. and Hashimoto T., *Phys. Rev. Lett.* **72** (1994) 2037.
[55] DeGroot J.V., Macosko C.W., Kume T. and Hashimoto T., *J. Colloid Interface Sci.* **166** (1994) 404.
[56] Boué F. and Lindner P., *Europhys. Lett.* **25** (1994) 421.
[57] Walker L.M. and Wagner N.J., *J. Rheol.* **38** (1994) 1525.
[58] Rabin Y. and Bruinsma R., *Europhys. Lett.* **20** (1992) 79.
[59] Onuki A., *J. Phys. II France* **2** (1992) 45.
[60] Hoffmann H., Munkert U., Thunig C. and Valiente M., *J. Colloid Interface Sci.* **163** (1994) 217.
[61] Hoffmann H., Thunig C., Schmiedel P. and Munkert U., *Langmuir* **10** (1994) 3972.
[62] Läuger J., Weigel R., Berger K., Hiltrop K. and Richtering W., submitted.